SPECTRUM BROADENING EFFECT IN COHERENT X-RAY RADIATION OF A RELATIVISTIC ELECTRON CROSSING A SINGLE-CRYSTAL PLATE

S. V. Blazhevich[1] and A. V. Noskov[2] UDC 537.8

Based on the dynamic diffraction theory [1], coherent x-ray radiation of a relativistic electron crossing a single-crystal plate at a constant velocity is considered in the Bragg geometry. In the general case of asymmetric reflection of the radiation from the target, expressions are derived for the spectral-angular distribution of parametric x-ray radiation (PXR) and diffraction transition radiation (DTR). For a fixed angle between the electron trajectory and the system of parallel atomic planes of the crystal (Bragg's angle) it is shown that a decrease in the angle of electron incidence on the crystal plate gives rise to a significant increase in the PXR and DTR spectra, and the causes for spectral broadening for each of these radiation mechanisms are different.

Keywords: relativistic electron, coherent x-ray radiation, asymmetric reflection, spectral-angular density.

INTRODUCTION

When a fast charged particle crosses a single crystal, its coulomb field is scattered on the system of parallel atomic planes of the crystal, generating PXR [2–4]. Dynamic effects in PXR were reported in [5–8] in a geometry of symmetric reflection, where PXR is generally formed due to the main branch of the solution to the dispersion equation for x-rays in a crystal. In the Bragg scattering geometry in the case of symmetric reflection, the surface of the crystal target is parallel to the diffracting crystal surfaces ($\delta = 0$). The influence of reflection asymmetry ($\delta \neq 0$) on the spectral-angular characteristics of PXR and DTR in the Bragg geometry for a semi-finite crystal was investigated in [9, 10], for the case of a plane-parallel plate – in [11] (transition radiation of a relativistic electron) and in [12] (diffraction transition radiation). More recently in [13] it was shown that in the Bragg geometry reflection asymmetry exerts a considerable influence both on characteristics of parametric x-ray radiation along the velocity of a relativistic electron and on the contributions to the forward PXR yield from the two branches of the dispersion equation solution.

In this work we present the results of further theoretical investigation of coherent x-ray radiation of a relativistic electron crossing a single-crystal plate of finite thickness in the Bragg scattering geometry, which were obtained for the general case of asymmetric reflection (arbitrary orientation angle δ of atomic planes of the crystal with respect to its surface). Based on the analytical expressions derived for the spectral-angular distribution of PXR and DTR, we address the contribution from each of the two branches of the dispersion equation solution in the crystal into the yield of parametric x-ray radiation for different observation angles θ and investigate the influence of the reflection asymmetry on the spectral width of PXR and DTR and interference of PXR and DTR of a relativistic electron.

SPECTRAL-ANGULAR DISTRIBUTION OF RADIATION

Let a fast charged particle cross a single-crystal plate at a constant velocity V (Fig. 1). Consider an equation for a Fourier image of the electromagnetic field

---

[1]Belgorod State University, Belgorod, Russia, e-mail: blazh@bsu.edu.ru, Belgorod University of Consumer Cooperatives, Belgorod, Russia. Translated from Izvestiya Vysshikh Uchebnykh Zavedenii, Fizika, No. 3, pp. 74–83, March, 2009. Original article submitted 17.04.08.

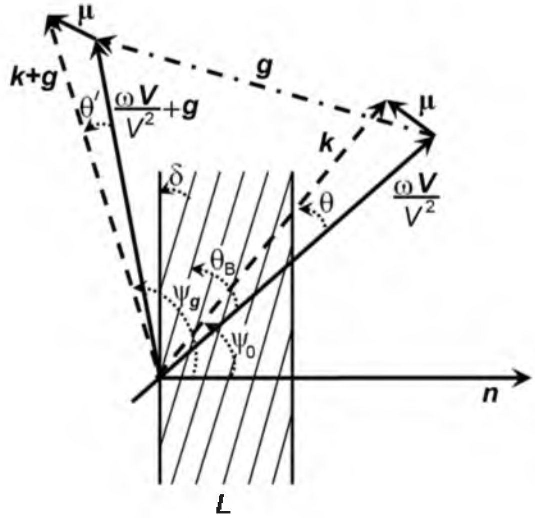

Fig. 1. Geometry of the radiation process.

$$\boldsymbol{E}(\boldsymbol{k},\omega)=\int dt\, d^3r\, \boldsymbol{E}(\boldsymbol{r},t)\exp(i\omega t-i\boldsymbol{kr})\,. \tag{1}$$

Since the field of a relativistic particle can be to a high accuracy taken to be transverse, the incident $\boldsymbol{E}_0(\boldsymbol{k},\omega)$ and diffracted $\boldsymbol{E}_g(\boldsymbol{k},\omega)$ electromagnetic waves would be described by two amplitudes with different values of transverse polarization

$$\begin{aligned}\boldsymbol{E}_0(\boldsymbol{k},\omega)&=E_0^{(1)}(\boldsymbol{k},\omega)\boldsymbol{e}_0^{(1)}+E_0^{(2)}(\boldsymbol{k},\omega)\boldsymbol{e}_0^{(2)},\\ \boldsymbol{E}_g(\boldsymbol{k},\omega)&=E_g^{(1)}(\boldsymbol{k},\omega)\boldsymbol{e}_1^{(1)}+E_g^{(2)}(\boldsymbol{k},\omega)\boldsymbol{e}_1^{(2)},\end{aligned} \tag{2}$$

where unit vectors $\boldsymbol{e}_0^{(1)}$ and $\boldsymbol{e}_0^{(2)}$ are perpendicular to vector $\boldsymbol{k}$, and unit vectors $\boldsymbol{e}_1^{(1)}$ and $\boldsymbol{e}_1^{(2)}$ are perpendicular to vector $\boldsymbol{k}_g=\boldsymbol{k}+\boldsymbol{g}$. Note that vectors $\boldsymbol{e}_0^{(2)}$, $\boldsymbol{e}_1^{(2)}$ lie in the plane of vectors $\boldsymbol{k}$ and $\boldsymbol{k}_g$ (π-polarization), and vectors $\boldsymbol{e}_0^{(1)}$ and $\boldsymbol{e}_1^{(1)}$ are perpendicular to it (σ - polarization), and $\boldsymbol{g}$ is the reciprocal lattice vector determining the system of reflecting atomic planes of the crystal. The system of equations for the Fourier image of the electromagnetic field in a two-wave approximation of the dynamic diffraction theory has the following form [14]:

$$\begin{cases}(\omega^2(1+\chi_0)-k^2)E_0^{(s)}+\omega^2\chi_{-g}C^{(s,\tau)}E_g^{(s)}=8\pi^2 ie\omega\theta VP^{(s)}\delta(\omega-\boldsymbol{kV}),\\ \omega^2\chi_g C^{(s,\tau)}E_0^{(s)}+(\omega^2(1+\chi_0)-k_g^2)E_g^{(s)}=0,\end{cases} \tag{3}$$

where $\chi_0=\chi_0'+i\chi_0''$ is the average dielectric susceptibility and χ_g, χ_{-g} are the coefficients of Fourier expansion of the dielectric susceptibility of the crystal over the reciprocal lattice vectors $\boldsymbol{g}$

$$\chi(\omega,\boldsymbol{r})=\sum_g \chi_g(\omega)e^{i\boldsymbol{gr}}=\sum_g\left(\chi_g'(\omega)+i\chi_g''(\omega)\right)e^{i\boldsymbol{gr}}\,. \tag{4}$$

Let us consider a crystal with a central symmetry $(\chi_{\boldsymbol{g}} = \chi_{-\boldsymbol{g}})$. In Eqs. (4), $\chi'_{\boldsymbol{g}}$ and $\chi''_{\boldsymbol{g}}$ are given by the following:

$$\chi'_{\boldsymbol{g}} = \chi'_0 \left(F(g)/Z\right)\left(S(\boldsymbol{g})/N_0\right)\exp\left(-\frac{1}{2}g^2u_\tau^2\right),\ \chi''_{\boldsymbol{g}} = \chi''_0 \exp\left(-\frac{1}{2}g^2u_\tau^2\right), \tag{5}$$

where $F(g)$ is the form factor of an atom containing Z electrons, $S(\boldsymbol{g})$ is the structural factor of a unit cell containing N_0 atoms, and u_τ is the root-mean-square amplitude of thermal vibrations of the crystal atoms. We consider an x-ray radiation region, for which $\chi'_{\boldsymbol{g}} < 0,\ \chi'_0 < 0$.

Quantities $C^{(s,\tau)}$ and $P^{(s)}$ are determined in the system of equations (3) as follows:

$$C^{(s,\tau)} = \boldsymbol{e}_0^{(s)}\boldsymbol{e}_1^{(s)} = (-1)^\tau C^{(s)},\ C^{(1)} = 1,\ C^{(2)} = \left|\cos 2\theta_B\right|,$$

$$P^{(s)} = \boldsymbol{e}_0^{(s)}(\boldsymbol{\mu}/\mu),\ P^{(1)} = \sin\varphi,\ P^{(2)} = \cos\varphi, \tag{6}$$

where $\boldsymbol{\mu} = \boldsymbol{k} - \omega\boldsymbol{V}/V^2$ is the component of the virtual photon momentum, which is perpendicular to the particle velocity $\boldsymbol{V}$ ($\mu = \omega\theta/V$, where $\theta \ll 1$ is the angle between $\boldsymbol{k}$ and $\boldsymbol{V}$), θ_B is the angle between the electron velocity and the system of crystallographic planes (Bragg angle), φ is the azimuthal radiation angle measured from the plane formed by vectors $\boldsymbol{V}$ and $\boldsymbol{g}$; the value of the reciprocal lattice vector is derived by the expression $g = 2\omega_B \sin\theta_B / V$, where ω_B is the Bragg frequency. The system of equations (3) for $s=1$ and $\tau=2$ describes the σ-polarized fields. For $s=2$, the system (3) describes the π-polarized fields, where if $2\theta_B < \frac{\pi}{2}$, then $\tau=2$, otherwise $\tau=1$.

Using standard methods of the dynamic theory [1], let us solve the following dispersion equation from the system of equations (3) for x-ray waves in the crystal:

$$(\omega^2(1+\chi_0) - k^2)(\omega^2(1+\chi_0) - k_{\boldsymbol{g}}^2) - \omega^4\chi_{-\boldsymbol{g}}\chi_{\boldsymbol{g}}C^{(s)2} = 0. \tag{7}$$

Find projections of the wave vectors $\boldsymbol{k}$ and $\boldsymbol{k}_{\boldsymbol{g}}$ given by

$$k_x = \omega\cos\psi_0 + \frac{\omega\chi_0}{2\cos\psi_0} + \frac{\lambda_0}{\cos\psi_0},\ k_{gx} = \omega\cos\psi_g + \frac{\omega\chi_0}{2\cos\psi_g} + \frac{\lambda_g}{\cos\psi_g}. \tag{8}$$

In so doing, we are going to make use of a well-known formula relating the additional dynamic terms λ_0 and $\lambda_{\boldsymbol{g}}$ [1]:

$$\lambda_{\boldsymbol{g}} = \frac{\omega\beta}{2} + \lambda_0\frac{\gamma_{\boldsymbol{g}}}{\gamma_0}, \tag{9}$$

where $\beta = \alpha - \chi_0\left(1 - \frac{\gamma_{\boldsymbol{g}}}{\gamma_0}\right)$, $\alpha = \frac{1}{\omega^2}(k_{\boldsymbol{g}}^2 - k^2)$, $\gamma_0 = \cos\psi_0$, $\gamma_{\boldsymbol{g}} = \cos\psi_{\boldsymbol{g}}$, ψ_0 is the angle between the incident wave vector $\boldsymbol{k}$ and the normal vector to the plate surface $\boldsymbol{n}$, and $\psi_{\boldsymbol{g}}$ is the angle between the wave vector $\boldsymbol{k}_{\boldsymbol{g}}$ and the normal vector. Scalars of vectors $\boldsymbol{k}$ and $\boldsymbol{k}_{\boldsymbol{g}}$ are equal

$$k = \omega\sqrt{1+\chi_0} + \lambda_0,\ k_{\boldsymbol{g}} = \omega\sqrt{1+\chi_0} + \lambda_{\boldsymbol{g}}. \tag{10}$$

Given that $k_{\parallel} \approx \omega \sin\psi_0$ and $k_{g\parallel} \approx \omega \sin\psi_g$, we obtain

$$\lambda_0^{(1,2)} = \omega \frac{\gamma_0}{4\gamma_g}\left(-\beta \pm \sqrt{\beta^2 + 4\chi_g \chi_{-g} C^{(s)^2} \frac{\gamma_g}{\gamma_0}}\right), \quad (11a)$$

$$\lambda_g^{(1,2)} = \frac{\omega}{4}\left(\beta \pm \sqrt{\beta^2 + 4\chi_g \chi_{-g} C^{(s)^2} \frac{\gamma_g}{\gamma_0}}\right). \quad (11b)$$

Since $|\lambda_0| << \omega$ and $|\lambda_g| << \omega$, it can be shown that $\theta \approx \theta'$ (see Fig. 1), therefore hereinafter θ' will be denoted as θ.

The solution to the first equation in the system (3) for an incident field in vacuum is given by

$$E_0^{(s)\mathrm{vac}} = \frac{8\pi^2 ieV\theta P^{(s)}}{\omega} \frac{1}{-\chi_0 - \frac{2}{\omega}\lambda_0} \delta\left(\lambda_0^* - \lambda_0\right) = \frac{8\pi^2 ieV\theta P^{(s)}}{\omega} \frac{1}{\frac{\gamma_0}{|\gamma_g|}\left(-\chi_0 - \frac{2}{\omega}\frac{\gamma_0}{\gamma_g}\lambda_g + \beta\frac{\gamma_0}{\gamma_g}\right)} \delta\left(\lambda_g^* - \lambda_g\right), \quad (12)$$

where $\lambda_g^* = \frac{\omega\beta}{2} + \frac{\gamma_g}{\gamma_0}\lambda_0^*$, $\lambda_0^* = \omega\left(\frac{\gamma^{-2} + \theta^2 - \chi_0}{2}\right)$, $\delta\left(\lambda_0^* - \lambda_0\right) = \frac{|\gamma_g|}{\gamma_0}\delta\left(\lambda_g^* - \lambda_g\right)$.

The solution to the system of equations (3) for the incident and diffracted fields in a crystal will, therefore, have the following form:

$$E_0^{(s)\mathrm{cr}} = \frac{8\pi^2 ieV\theta P^{(s)}}{\omega} \frac{2\omega\lambda_g}{4\frac{\gamma_0^2}{\gamma_g^2}\left(\lambda_g - \lambda_g^{(1)}\right)\left(\lambda_g - \lambda_g^{(2)}\right)} \delta\left(\lambda_g^* - \lambda_g\right)$$
$$+ \frac{2\omega\lambda_g}{\omega^2 \chi_g C^{(s,\tau)}} E^{(s)(1)} \delta(\lambda_g - \lambda_g^{(1)}) + \frac{2\omega\lambda_g}{\omega^2 \chi_g C^{(s,\tau)}} E^{(s)(2)} \delta(\lambda_g - \lambda_g^{(2)}), \quad (13)$$

$$E_g^{(s)\mathrm{cr}} = \frac{8\pi^2 ieV\theta P^{(s)}}{\omega} \frac{\omega^2 \chi_g C^{(s,\tau)}}{4\frac{\gamma_0^2}{\gamma_g^2}\left(\lambda_g - \lambda_g^{(1)}\right)\left(\lambda_g - \lambda_g^{(2)}\right)} \delta\left(\lambda_g^* - \lambda_g\right)$$
$$+ E^{(s)(1)} \delta(\lambda_g - \lambda_g^{(1)}) + E^{(s)(2)} \delta(\lambda_g - \lambda_g^{(2)}), \quad (14)$$

where $E^{(s)(1)}$ and $E^{(s)(2)}$ are the free fields corresponding to the two solutions (11b) of the dispersion equation (7).

The diffracted field in vacuum is given by

$$E_g^{(s)\mathrm{vac}} = E_{\mathrm{Rad}}^{(s)} \delta\left(\lambda_g + \frac{\omega\chi_0}{2}\right), \quad (15)$$

where $E_{\mathrm{Rad}}^{(s)}$ is the sought-for radiation field.

The expression relating the diffracted and incident fields in the crystal follows from the second equation of the system (3)

$$E_0^{(s)\mathrm{cr}} = \frac{2\omega\lambda_{\boldsymbol{g}}}{\omega^2 \chi_{\boldsymbol{g}} C^{(s,\tau)}} E_{\boldsymbol{g}}^{(s)\mathrm{cr}} . \tag{16}$$

Making use of ordinary boundary conditions on the input and output surfaces of the crystal plate

$$\int E_0^{(s)\mathrm{vac}}\, d\lambda_{\boldsymbol{g}} = \int E_0^{(s)\mathrm{cr}}\, d\lambda_{\boldsymbol{g}} , \tag{17a}$$

$$\int E_{\boldsymbol{g}}^{(s)\mathrm{cr}}\, d\lambda_{\boldsymbol{g}} = \int E_{\boldsymbol{g}}^{(s)\mathrm{vac}}\, d\lambda_{\boldsymbol{g}} , \tag{17b}$$

$$\int E_{\boldsymbol{g}}^{(s)\mathrm{cr}} e^{i\frac{\lambda_{\boldsymbol{g}}}{\gamma_{\boldsymbol{g}}}L}\, d\lambda_{\boldsymbol{g}} = 0 , \tag{17c}$$

we obtain an expression for the radiation field

$$E_{\mathrm{Rad}}^{(s)} = \frac{8\pi^2 ieV\theta P^{(s)}}{\omega} \frac{\omega^2 \chi_{\boldsymbol{g}} C^{(s,\tau)}}{2\omega\left(\lambda_{\boldsymbol{g}}^{(2)} e^{i\frac{\lambda_{\boldsymbol{g}}^* - \lambda_{\boldsymbol{g}}^{(2)}}{\gamma_{\boldsymbol{g}}}L} - \lambda_{\boldsymbol{g}}^{(1)} e^{i\frac{\lambda_{\boldsymbol{g}}^* - \lambda_{\boldsymbol{g}}^{(1)}}{\gamma_{\boldsymbol{g}}}L}\right)}$$

$$\times\left[\left(\frac{1}{\frac{\gamma_0}{|\gamma_{\boldsymbol{g}}|}\left(-\chi_0 - \frac{2}{\omega}\frac{\gamma_0}{\gamma_{\boldsymbol{g}}}\lambda_{\boldsymbol{g}}^* + \beta\frac{\gamma_0}{\gamma_{\boldsymbol{g}}}\right)} - \frac{2\omega e^{i\frac{\lambda_{\boldsymbol{g}}^* - \lambda_{\boldsymbol{g}}^{(2)}}{\gamma_{\boldsymbol{g}}}L}}{4\frac{\gamma_0^2}{\gamma_{\boldsymbol{g}}^2}\left(\lambda_{\boldsymbol{g}}^* - \lambda_{\boldsymbol{g}}^{(1)}\right)}\right)\left(1 - e^{i\frac{\lambda_{\boldsymbol{g}}^* - \lambda_{\boldsymbol{g}}^{(1)}}{\gamma_{\boldsymbol{g}}}L}\right)\right. \tag{18}$$

$$\left. - \left(\frac{1}{\frac{\gamma_0}{|\gamma_{\boldsymbol{g}}|}\left(-\chi_0 - \frac{2}{\omega}\frac{\gamma_0}{\gamma_{\boldsymbol{g}}}\lambda_{\boldsymbol{g}}^* + \beta\frac{\gamma_0}{\gamma_{\boldsymbol{g}}}\right)} - \frac{2\omega e^{i\frac{\lambda_{\boldsymbol{g}}^* - \lambda_{\boldsymbol{g}}^{(1)}}{\gamma_{\boldsymbol{g}}}L}}{4\frac{\gamma_0^2}{\gamma_{\boldsymbol{g}}^2}\left(\lambda_{\boldsymbol{g}}^* - \lambda_{\boldsymbol{g}}^{(2)}\right)}\right)\left(1 - e^{i\frac{\lambda_{\boldsymbol{g}}^* - \lambda_{\boldsymbol{g}}^{(2)}}{\gamma_{\boldsymbol{g}}}L}\right)\right].$$

Since the radiation field contains contributions from PXR and DTR, let us represent the amplitude $E_{\mathrm{Rad}}^{(s)}$ as a sum of the PXR and DTR amplitudes

$$E_{\mathrm{Rad}}^{(s)} = E_{\mathrm{PXR}}^{(s)} + E_{\mathrm{DTR}}^{(s)} , \tag{19}$$

where

$$E_{\mathrm{PXR}}^{(s)} = \frac{8\pi^2 ieV\theta P^{(s)}}{\omega} \frac{\omega^2 \chi_{\boldsymbol{g}} C^{(s,\tau)}}{2\omega\left(\lambda_{\boldsymbol{g}}^{(2)} e^{i\frac{\lambda_{\boldsymbol{g}}^* - \lambda_{\boldsymbol{g}}^{(2)}}{\gamma_{\boldsymbol{g}}}L} - \lambda_{\boldsymbol{g}}^{(1)} e^{i\frac{\lambda_{\boldsymbol{g}}^* - \lambda_{\boldsymbol{g}}^{(1)}}{\gamma_{\boldsymbol{g}}}L}\right)}$$

$$\times\left[\left(\frac{2\omega e^{i\frac{\lambda_g^*-\lambda_g^{(1)}}{\gamma_g}L}}{4\frac{\gamma_0^2}{\gamma_g^2}\left(\lambda_g^*-\lambda_g^{(2)}\right)}+\frac{\omega}{2\frac{\gamma_0}{|\gamma_g|}\lambda_0^*}\right)\left(1-e^{i\frac{\lambda_g^*-\lambda_g^{(2)}}{\gamma_g}L}\right)\right.$$

$$\left.-\left(\frac{2\omega e^{i\frac{\lambda_g^*-\lambda_g^{(2)}}{\gamma_g}L}}{4\frac{\gamma_0^2}{\gamma_g^2}\left(\lambda_g^*-\lambda_g^{(1)}\right)}+\frac{\omega}{2\frac{\gamma_0}{|\gamma_g|}\lambda_0^*}\right)\left(1-e^{i\frac{\lambda_g^*-\lambda_g^{(1)}}{\gamma_g}L}\right)\right], \tag{20}$$

$$E_{\mathrm{DTR}}^{(s)}=\frac{8\pi^2 ieV\theta P^{(s)}}{\omega}\frac{\omega^2\chi_g C^{(s,\tau)}}{2\omega\left(\lambda_g^{(2)}e^{-i\frac{\lambda_g^{(2)}}{\gamma_g}L}-\lambda_g^{(1)}e^{-i\frac{\lambda_g^{(1)}}{\gamma_g}L}\right)}$$

$$\times\left[\frac{1}{\frac{\gamma_0}{|\gamma_g|}\left(-\chi_0-\frac{2}{\omega}\frac{\gamma_0}{\gamma_g}\lambda_g^*+\beta\frac{\gamma_0}{\gamma_g}\right)}+\frac{\omega}{2\frac{\gamma_0}{|\gamma_g|}\lambda_0^*}\right]\left(e^{-i\frac{\lambda_g^{(2)}}{\gamma_g}L}-e^{-i\frac{\lambda_g^{(1)}}{\gamma_g}L}\right). \tag{21}$$

Expression (20) describes the PXR field. The branch of PXR, for which the real part of the denominator can vanish to zero $\mathrm{Re}\left(\lambda_g^*-\lambda_g^{(1,2)}\right)=0$, is significant. It was assumed earlier that only one branch makes a significant contribution to the PXR yield [8]. The cited work, however, addresses a particular case of symmetric reflection, where the atomic planes are parallel to the crystal plate surface $\left(\frac{|\gamma_g|}{\gamma_0}=1\right)$. In this work, we consider a general asymmetric case, so in what follows we are going to point out the conditions under which the other PXR branch predominates.

For further analysis, it is reasonable to represent λ_g^* and $\lambda_g^{(1,2)}$ as

$$\lambda_g^{(1,2)}=\frac{\omega\left|\chi_g' C^{(s)}\right|}{2}\left(\xi^{(s)}-\frac{i\rho^{(s)}(1+\varepsilon)}{2}\right.$$
$$\left.\pm\sqrt{\xi^{(s)2}-\varepsilon-i\rho^{(s)}((1+\varepsilon)\xi^{(s)}-2\kappa^{(s)}\varepsilon)-\rho^{(s)2}\left(\frac{(1+\varepsilon)^2}{4}-\kappa^{(s)2}\varepsilon\right)}\right), \tag{22a}$$

$$\lambda_g^*=\frac{\omega\left|\chi_g' C^{(s)}\right|}{2}\left(2\xi^{(s)}-i\rho^{(s)}-\varepsilon\sigma^{(s)}\right), \tag{22b}$$

where

$$\xi^{(s)}(\omega)=\frac{\alpha}{2|\chi_g' C^{(s)}|}-\frac{\chi_0'(1+\varepsilon)}{2|\chi_g' C^{(s)}|}=\eta^{(s)}(\omega)+\frac{(1+\varepsilon)}{2\nu^{(s)}},\ \nu^{(s)}=\frac{|\chi_g' C^{(s)}|}{|\chi_0'|},\ \rho^{(s)}=\frac{\chi_0''}{|\chi_g' C^{(s)}|},$$

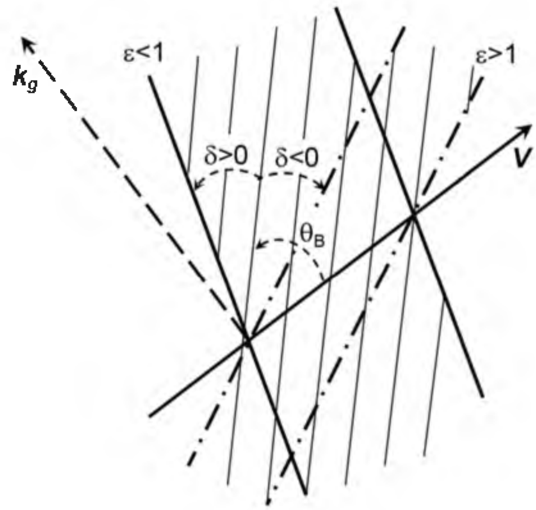

Fig. 2. Two possible orientations of the plate surface for a fixed angle θ_B.
The first one corresponds to $\varepsilon < 1$, the second one corresponds to $\varepsilon > 1$.

$$\eta^{(s)}(\omega) = \frac{\alpha}{2|\chi'_g C^{(s)}|} = \frac{2\sin^2\theta_B}{V^2|\chi'_g C^{(s)}|}\left(\frac{\omega_B(1+\theta\cos\varphi\cot\theta_B)}{\omega} - 1\right), \ \varepsilon = \frac{|\gamma_g|}{\gamma_0}, \ \kappa^{(s)} = \frac{\chi''_g C^{(s)}}{\chi''_0},$$

$$\sigma^{(s)} = \frac{1}{|\chi'_g| C^{(s)}}\left(\theta^2 + \gamma^{-2} - \chi'_0\right). \qquad (23)$$

Since in the region of resonant frequencies the inequality $2\sin^2\theta_B / V^2|\chi'_g| C^{(s)} >> 1$ is fulfilled, so $\eta^{(s)}(\omega)$ is a fast function of frequency ω, and for further analysis of the PXR and DTR properties it is convenient to treat $\eta^{(s)}(\omega)$ as a spectral variable characterizing the frequency ω. Note that the resulting formulas contain $\xi^{(s)}(\omega) = \eta^{(s)}(\omega) + \frac{(1+\varepsilon)}{2\nu^{(s)}}$ instead of $\eta^{(s)}(\omega)$, where the second term in the former expression is due to the refraction effect.

When deriving Eqs. (22), we took into consideration that in the radiation geometry under study the angle between the diffracted photon momentum and the normal vector to the crystal surface is obtuse, implying that $\gamma_g = \cos\psi_g < 0$.

Parameter ε from Eq. (23) can be given by $\varepsilon = \sin(\theta_B - \delta)/\sin(\theta_B + \delta)$, where δ is the angle between the input surface of the target and the crystallographic plane. For a fixed angle θ_B the value of ε determines orientation of the input crystal plate surface with respect of the system of diffracting atomic planes (Fig. 2). With decreasing the angle $(\theta_B + \delta)$ of electron incidence on the target, parameter δ becomes negative and further its scalar value is increased (in the limiting case $\delta \to -\theta_B$), which results in increasing ε. On the contrary, when the angle of incidence is increased, ε decreases (the limiting case is $\delta \to \theta_B$).

EFFECT OF RELECTION ASYMMETRY ON PXR AND DTR SPECTRA

Let us consider a thin crystal and disregard absorption, assuming that $\rho^{(s)} = 0$. Substituting Eqs. (20) and (21) into a well-known expression [14] for the spectral-angular x-ray radiation density

$$\omega \frac{d^2 N}{d\omega d\Omega} = \omega^2 (2\pi)^{-6} \sum_{s=1}^{2} \left| E_{\text{Rad}}^{(s)} \right|^2 , \tag{24}$$

we obtain an expression for the spectral-angular PXR and DTR distribution

$$\omega \frac{d^2 N_{\text{PXR}}^{(s)}}{d\omega d\Omega} = \frac{e^2}{\pi^2} \frac{P^{(s)^2} \theta^2}{(\theta^2 + \gamma^{-2} - \chi_0')^2} \left(R_{\text{PXR}}^{(1)^{(s)}} + R_{\text{PXR}}^{(2)^{(s)}} + R^{\text{INT}^{(s)}} \right),$$

$$R_{\text{PXR}}^{(1)^{(s)}} = \left| \frac{\Omega_+^{(s)}}{\Delta^{(s)}} \frac{1 - e^{-ib^{(s)}\left(\Delta_+^{(s)} - \sigma^{(s)}\right)}}{\Delta_+^{(s)} - \sigma^{(s)}} \right|^2 , \quad R_{\text{PXR}}^{(2)^{(s)}} = \left| \frac{\Omega_-^{(s)}}{\Delta^{(s)}} \frac{1 - e^{-ib^{(s)}\left(\Delta_-^{(s)} - \sigma^{(s)}\right)}}{\Delta_-^{(s)} - \sigma^{(s)}} \right|^2 , \tag{25a}$$

$$R_{\text{INT}}^{(1,2)^{(s)}} = -2 \operatorname{Re} \left(\left(\frac{\Omega_+^{(s)}}{\Delta^{(s)}} \frac{1 - e^{-ib^{(s)}\left(\Delta_+^{(s)} - \sigma^{(s)}\right)}}{\Delta_+^{(s)} - \sigma^{(s)}} \right) \left(\frac{\Omega_-^{(s)}}{\Delta^{(s)}} \frac{1 - e^{-ib^{(s)}\left(\Delta_-^{(s)} - \sigma^{(s)}\right)}}{\Delta_-^{(s)} - \sigma^{(s)}} \right)^* \right), \tag{25b}$$

$$\omega \frac{d^2 N_{\text{DTR}}^{(s)}}{d\omega d\Omega} = \frac{e^2}{\pi^2} P^{(s)^2} \theta^2 \left(\frac{1}{\theta^2 + \gamma^{-2} - \chi_0'} - \frac{1}{\theta^2 + \gamma^{-2}} \right)^2 R_{\text{DTR}}^{(s)},$$
$$R_{\text{DTR}}^{(s)} = \left| \frac{e^{ib^{(s)}\Delta_-^{(s)}} - e^{ib^{(s)}\Delta_+^{(s)}}}{\Delta_-^{(s)} e^{ib^{(s)}\Delta_-^{(s)}} - \Delta_+^{(s)} e^{ib^{(s)}\Delta_+^{(s)}}} \right|^2 , \tag{25c}$$

where the following notations have been introduced:

$$\Delta^{(s)} = \Delta_-^{(s)} e^{-ib^{(s)}\Delta_+^{(s)}} - \Delta_+^{(s)} e^{-ib^{(s)}\Delta_-^{(s)}} , \quad \Omega_\pm^{(s)} = \sigma^{(s)} \left(e^{-ib^{(s)}\Delta_\mp^{(s)}} - 1 \right) + \Delta_\pm^{(s)} ,$$

$$\Delta_\pm^{(s)} = \frac{\xi^{(s)} \pm \sqrt{\xi^{(s)^2} - \varepsilon}}{\varepsilon} , \quad b^{(s)} = \frac{\omega \left| \chi_g' C^{(s)} \right| L}{2\gamma_0} .$$

Note that parameter $b^{(s)}$ is equal to the ratio of a half of the electron path length in the plate $L / 2\gamma_0$ to the x-ray extinction length in the crystal $1/\omega \left| \chi_g' C^{(s)} \right|$.

Function $R_{\text{PXR}}^{(1)^{(s)}}$ describes the spectrum corresponding to the first branch of PXR, $R_{\text{PXR}}^{(2)^{(s)}}$ describes the second branch, and $R^{\text{INT}^{(s)}}$ is the result of interference of the two x-ray waves corresponding to them. The above expressions, Eqs. (25), obtained following the dynamic diffraction theory for the spectral-angular density of the two branches of PXR and DTR represent the main result of this study.

A contribution from the first (or second) branch would be significant, when the respective equations are solved

$$\Delta_+^{(s)} - \sigma^{(s)} = \frac{\xi^{(s)} + \sqrt{\xi^{(s)2} - \varepsilon}}{\varepsilon} - \sigma^{(s)} = 0 , \tag{26a}$$

$$\Delta_-^{(s)} - \sigma^{(s)} = \frac{\xi^{(s)} - \sqrt{\xi^{(s)2} - \varepsilon}}{\varepsilon} - \sigma^{(s)} = 0 . \tag{26b}$$

As follows from Eq. (26), the maximum of the PXR spectrum always lies outside the region of total reflection (extinction)

$$\xi^{(s)} = \sqrt{\varepsilon} + \frac{\left(\sigma^{(s)}\sqrt{\varepsilon}-1\right)^2}{2\sigma^{(s)}} > \sqrt{\varepsilon}\,. \qquad (26c)$$

The region of total reflection is determined by the following inequality:

$$-\sqrt{\varepsilon} - \frac{1+\varepsilon}{2\nu^{(s)}} < \eta^{(s)} < \sqrt{\varepsilon} - \frac{1+\varepsilon}{2\nu^{(s)}}\,. \qquad (26d)$$

Extinction occurs in the case where a double-reflected wave coincides with the primary wave in its direction, but is phase-delayed by π with respect to it. Due to this fact, the incident wave amplitude in the course of wave propagation into the bulk of the crystal would decrease, implying that its energy would be transferring into the reflected wave [1].

It is evident that the width of this region is controlled by $2\sqrt{\varepsilon}$.

It can be demonstrated that Eq. (26a) can be solved given that

$$\varepsilon > \frac{1}{\sigma^{(s)2}} \text{ or } \varepsilon > \frac{\nu^{(s)2}}{\left(\frac{\theta^2}{|\chi_0'|} + \frac{1}{\gamma^2|\chi_0'|} + 1\right)^2}, \qquad (27a)$$

Eq. (26b) is solvable only if

$$\varepsilon < \frac{1}{\sigma^{(s)2}} \text{ or } \varepsilon < \frac{\nu^{(s)2}}{\left(\frac{\theta^2}{|\chi_0'|} + \frac{1}{\gamma^2|\chi_0'|} + 1\right)^2}\,. \qquad (27b)$$

Parameter $\nu^{(s)} = \frac{|\chi_g' C^{(s)}|}{|\chi_0'|}$ in the case of strong reflection of x-ray waves from atomic planes is close to unity, while in the case of weak reflections it is close to zero. Since $\nu^{(s)} < 1$, then in the case where $\varepsilon \geq \nu^{(s)2}$, only the inequality (27a) is satisfied, implying that in this case only Eq. (26a) is solvable, and it is the first branch $R_{\text{PXR}}^{(1)(s)}$ that contributes to the PXR yield. Should we increase the reflection asymmetry so that parameter ε would grow, then the spectral width would increase as well (Fig. 3). Indeed, the larger the parameter ε, the weaker the denominator $\Delta_+^{(s)} - \sigma^{(s)}$ in the expression for the $R_{\text{PXR}}^{(1)(s)}$ spectrum would vary with $\xi^{(s)}(\omega)$.

It should be noted that the electron path length in the crystal plate L/γ_0 remains unchanged for a constant value of parameter $b^{(s)}$. If we consider a case where $\varepsilon < \nu^{(s)2}$, then, depending on the observation angle θ and the electron energy γ, either of the inequalities, Eq. (27a) or Eq. (27b), is satisfied, hence, for a fixed electron energy and the same observation angles θ, the first PXR branch can predominate (Fig. 4), while for other values it would be the second branch (Fig. 5). A narrower PXR spectrum would correspond to smaller values of parameter ε.

Let us consider now the effect of reflection asymmetry on the DTR spectrum. The curves of spectral dependence $R_{\text{DTR}}^{(s)}$ constructed following Eq. (25c) are depicted in Fig. 6 and exhibit a strong effect of reflection asymmetry on the spectrum of DTR. It is evident that an increase in parameter ε gives rise to an increase in the spectral width, which is associated with the respective increase in the region of total reflection (extinction) (see Eq. (26d). Note

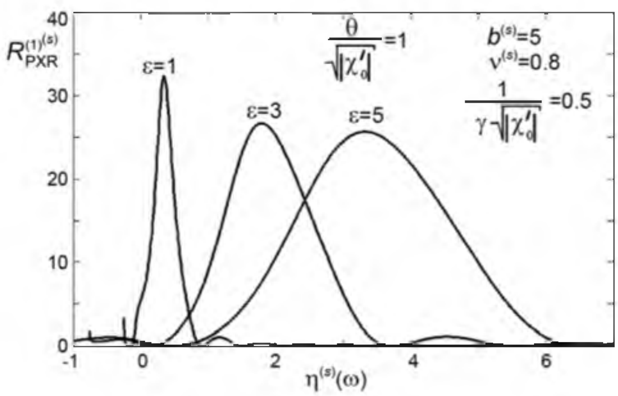

Fig. 3. Effect of reflection asymmetry on the PXR spectral width.

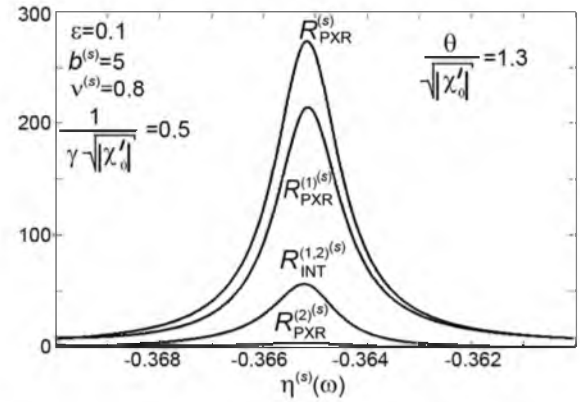

Fig. 4. Spectra of two PXR branches.

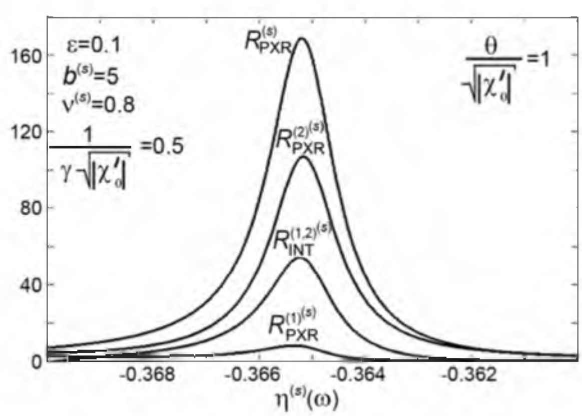

Fig. 5. Spectra of two PXR branches.

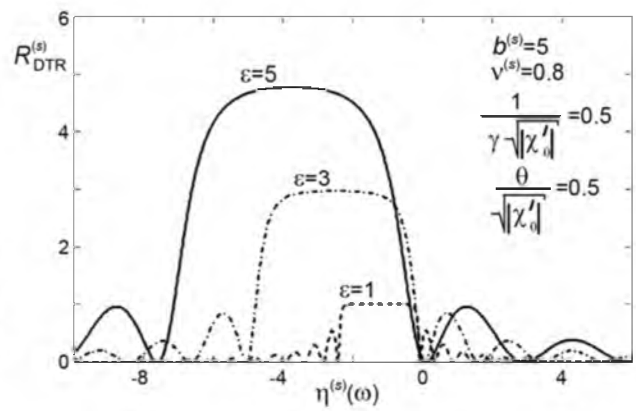

Fig. 6. Effect of asymmetry on the DTR spectrum.

that the spectral amplitude is also significantly increased, which is due to proportionality of the incident field amplitude to the value of $\varepsilon = \frac{|\gamma_g|}{\gamma_0}$ (see. Eq.(12)) in the case of diffraction.

ANGULAR DENSITY OF PXR AND DTR

In order to analyze the effect of asymmetry on the angular density of radiation, let us integrate Eq. (25) with respect to the function $\eta^{(s)}(\omega)$ and write an equation for the angular density of PXR and DTR and their interference term, which determines the total radiation density

$$\frac{dN_{\mathrm{PXR,DTR,INT}}^{(s)}}{d\Omega} = \frac{e^2 \nu^{(s)} P^{(s)^2}}{2\pi^2 \sin^2\theta_B} F_{\mathrm{PXR,DTR,INT}}^{(s)}, \tag{28a}$$

$$F_{\mathrm{PXR}}^{(s)}=\frac{\dfrac{\theta^2}{|\chi_0'|}}{\left(\dfrac{\theta^2}{|\chi_0'|}+\dfrac{1}{\gamma^2|\chi_0'|}+1\right)^2}\int\limits_{-\infty}^{\infty}\left(R_{\mathrm{PXR}}^{(1)(s)}+R_{\mathrm{PXR}}^{(2)(s)}+R^{\mathrm{INT}(s)}\right)d\eta^{(s)}, \tag{28b}$$

$$F_{\mathrm{DTR}}^{(s)}=\frac{\dfrac{\theta^2}{|\chi_0'|}}{\left(\dfrac{\theta^2}{|\chi_0'|}+\dfrac{1}{\gamma^2|\chi_0'|}+1\right)^2\left(\dfrac{\theta^2}{|\chi_0'|}+\dfrac{1}{\gamma^2|\chi_0'|}\right)^2}\int\limits_{-\infty}^{\infty}R_{\mathrm{DTR}}^{(s)}d\eta^{(s)}, \tag{28c}$$

$$F_{\mathrm{INT}}^{(s)}=-2\frac{\dfrac{\theta^2}{|\chi_0'|}}{\left(\dfrac{\theta^2}{|\chi_0'|}+\dfrac{1}{\gamma^2|\chi_0'|}+1\right)^2\left(\dfrac{\theta^2}{|\chi_0'|}+\dfrac{1}{\gamma^2|\chi_0'|}\right)} \tag{28d}$$

$$\times\int\limits_{-\infty}^{\infty}\mathrm{Re}\left(\left(\frac{\Omega_+^{(s)}}{\Delta^{(s)}}\frac{1-e^{-ib^{(s)}\left(\Delta_+^{(s)}-\sigma^{(s)}\right)}}{\Delta_+^{(s)}-\sigma^{(s)}}-\frac{\Omega_-^{(s)}}{\Delta^{(s)}}\frac{1-e^{-ib^{(s)}\left(\Delta_-^{(s)}-\sigma^{(s)}\right)}}{\Delta_-^{(s)}-\sigma^{(s)}}\right)\left(\frac{e^{ib^{(s)}\Delta_-^{(s)}}-e^{ib^{(s)}\Delta_+^{(s)}}}{\Delta_-^{(s)}e^{ib^{(s)}\Delta_-^{(s)}}-\Delta_+^{(s)}e^{ib^{(s)}\Delta_+^{(s)}}}\right)^*\right)d\eta^{(s)}.$$

Figures 7–9 depict the curves describing contributions from PXR, DTR and their interference term into the total angular density $F^{(s)}=F_{\mathrm{PXR}}^{(s)}+F_{\mathrm{DTR}}^{(s)}+F_{\mathrm{INT}}^{(s)}$, which were constructed according to Eqs.(28) for specific values of crystal parameters and electron energy. It is evident from Figs. 7 and 8 that with decreasing the angle of electron incidence on the plate (increasing parameter ε) there is a considerable increase in the angular PXR and DTR density and the total angular density of radiation. Expression (28) allows us to study the dependence of the angular density of radiation on the incident electron energy. For comparison, Fig. 9 depicts the curves of the angular density distribution for the same parameters as in Fig. 8 but for larger electron energies. It is clear that in this case the diffraction transition radiation contributes more significantly into the total angular density than does the parametric x-ray radiation.

SUMMARY

Based on the dynamic diffraction theory, analytical expressions have been derived in this work for the spectral-angular distribution of parametric x-ray radiation and diffraction transition radiation of a relativistic electron crossing a single-crystal plate in the Bragg scattering geometry in the general case of symmetric reflection. The contributions into PXR from the two branches of the solution to the dispersion equation for x-ray waves in a crystal have been examined. It has been shown here that for the case of electron incidence on the plate at a large angle to its surface the ratio of the contributions from the two branches will sharply vary with the observation angle θ.

With a decrease in the angle of electron incidence on the crystal plate and unvaried Bragg angle, the PXR spectral width is considerably increased, which gives rise to increased angular density (the effect is not due to absorption). Also, the influence of reflection asymmetry on the diffraction transition radiation spectrum has been studied. It has been demonstrated that with a decrease in the angle of surface orientation with respect to the system of crystallographic planes δ, both the spectral width and amplitude of DTR are increased. The dependences of relative contributions from PXR, DTR and their interference term into the total angular density on reflection asymmetry have been investigated.

This study has been performed using an RFBR grant (Project No. 08-02-12015-ofi) and a BelSU grant ВКГ 001-08.

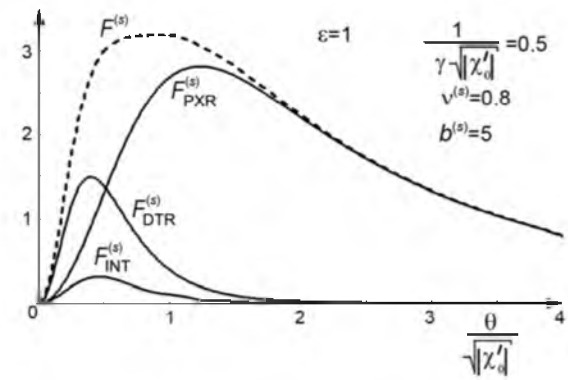

Fig. 7

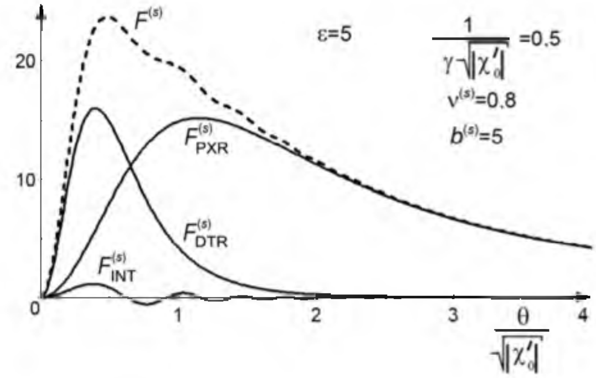

Fig. 8

Fig. 7. Angular density of radiation in a symmetrical case.

Fig. 8. Angular density of radiation in an asymmetrical case.

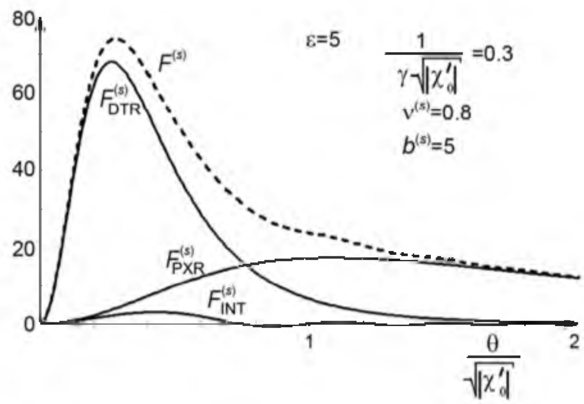

Fig. 9. Angular density of radiation in an asymmetrical case for higher electron energy than in Fig. 8.

REFERENCES

1. Z. G. Pinsker, Dynamic X-Ray Scattering in Perfect Crystals [in Russian], Moscow, Nauka (1974).
2. M. L. Ter-Mikaelyan, Effects of Environment on Electromagnetic Properties at High Energies [in Russian], Akad. Nauk. Arm. SSR (1969).
3. G. M. Garibyan and Yan Shi, Zh. Exp. Teor. Fiz., **63**, No. 4, 1198 (1972).
4. V. G. Baryshevskii and I. D. Feranchuk, *Ibid.*, 944.
5. N. Nasonov, A. Noskov, *et al.*, Rus. Phys. J, No. 6, 651–660 (2001).
6. A. S. Kubankin, N. N. Nasonov, V. I. Sergienko, and I. E. Vnukov, Nucl. Instr. and Meth. B, **201**, 97 (2003).
7. Yu. N. Adischev, S. N. Arishev, A. V. Vnukov, *et al.*, *Ibid.*, **201**, 114 (2003).
8. N. N. Nasonov, V. V. Kaplin, S. R. Uglov, *et al.*, *Ibid.*, **227**, 41 (2005).
9. S. V. Blazhevich and A. V. Noskov, X-Ray, Synchrotron and Neutron Studies [in Russian], No. 4, 23 (2006).
10. S. V. Blazhevich and A. V. Noskov, *Ibid.*, No. 4, 62 (2007).

11. S. V. Blazhevich and A. V. Noskov, Rus. Phys. J., No. 6, **49,** 606–612 (2006).
12. S. Blazhevich and A. Noskov, Nucl. Instr. Meth.B, **252**, 69 (2006).
13. S. V. Blazhevich and A. V. Noskov, Rus. Phys. J., No. 6, 574–585 (2007).
14. V. A. Bazylev and N. K. Zhevago, Radiation of Fast Particles in Matter and External Fields [in Russian], Moscow, Nauka (1987).